

Activation of organoclays and preparation of polyethylene nanocomposites

David J. Chaiko*

Argonne National Laboratory, Chemical Engineering Division,9700 South Cass Avenue, Argonne, IL 60439; Fax 312-413-2279; Chaiko@comcast.net

(Received: 9 November, 2005; published: 18 May, 2006)

Abstract: A dimethyl dihydrogenated tallow ammonium bentonite, edge modified with 1-hydroxydodecane-1,1-diphosphonic acid, was activated by intercalation of polyethylene-block-poly(ethylene glycol). A high-density polyethylene (HDPE) nanocomposite was produced by the gradual dilution of the intercalated organoclay with HDPE, via melt mixing, until a final clay concentration of 0.3 wt% was reached. While polymer crystallinity was unaffected by the addition of the clay, polymer transparency increased dramatically. Microscopic examination of compression molded films verified that polymer nucleation increased to such an extent that the normal spherulitic structure was completely absent. A significant reduction in gas transmission accompanied the increased film clarity. Compared to the pure polymer, oxygen and water vapor permeabilities were reduced by approximately 55 and 70%, respectively. With proper dispersion, significant improvements in both physical and barrier properties are achievable by the incorporation of nanoclays into polyolefins. Additionally, it is significant that these benefits can be realized at clay concentrations consistent with those of common polymer additives, like stabilizers, clarifiers, and colorants.

Introduction

First attempts to enhance the dispersion of smectite clays into polymers, through modification of the mineral surface with surfactants, date back to the work of Jordan and his colleagues in the 1940s [1-4]. While their pioneering efforts failed to yield commercial nanocomposite products, their decade-long effort did lead to the development of organoclay technologies that became a mainstay for rheology control in solvent-based paints, drilling fluids, and high-temperature greases for over six decades. Those first efforts by Jordan have prompted many others [5,6] to consider surface-treated clays as functional fillers for polymers, and eventually led to the commercial introduction of nylon nanocomposites by Toyota [7,8] in the 1980s. Since then, nanoclay technologies have encompassed a wide range of thermoplastic and thermoset polymers with improved properties, such as mechanical strength, gas barrier, chemical resistance, and flame

_

^{*} Current affiliation: Adjunct Professor, University of Illinois at Chicago, Department of Earth and Environmental Sciences, 845 West Taylor St., Chicago, IL 60607.

retardancy. Unfortunately, the property improvements have not always lived up to expectations.

Much of contemporary nanoclay technology bears a great deal of similarity to the original chemistries and dispersion methods developed by Jordan [2-4]. He discovered that the degree of organoclay swelling and exfoliation in solvents could be greatly improved by the addition of moderate amounts of polar activators. Activators, such as acetone, methanol, and ethanol, greatly increased the degree of organoclay exfoliation in nonpolar solvents like toluene and xylene. In clay/polymer applications, oligomers [9-11] and copolymers [12] have replaced the volatile swelling agents used by Jordan. But this approach has not been fully satisfactory. For example, there are still no reports in the literature of increased water vapor barrier being achieved by the dispersion of organoclays in polyolefin homopolymers.

In the present study, solvent/activator systems were used to prepare organoclays intercalated with polyethylene-block-poly(ethylene glycol). Nanoclay dispersion into high-density polyethylene (HDPE) was performed by using a gradual dilution technique, whereby initial polymer additions to the intercalate were made under conditions such that the nanoclay was the continuous phase. HDPE was chosen for this study because it has (a) extremely rapid crystallization kinetics, (b) a high degree of crystallinity, and (c) the lowest water vapor transmission rate (WVTR) of all of the polyethylenes. As such, it represents the greatest challenge towards increasing nucleation density and gas barrier (e.g., water vapor) through the application of nanotechnology.

Results and discussion

Organoclay activation

The first published papers [2-4] on organoclays provided details on the use of polar activators to promote exfoliation of organoclays in nonpolar solvents like toluene. In retrospect, it is fair to say that the most effective activators were low-molecular-weight molecules that happen to possess both a high dipole moment and high permittivity (i.e., nitrobenzene, methanol, acetone). As a class, the best activators can be characterized as molecules that are (a) able to diffuse rapidly into the organoclay galleries, (b) able to solvate both polar and nonpolar sites on the clay surface, (c) incapable of interacting with more than one clay platelet at a time, and (d) miscible with the wetting solvent.

The organoclay literature on activator use can be somewhat misleading regarding recommendations on the amount of activator that should be used. For example, the *Rheology Handbook* provided by Elementis (Hightstown, NJ) suggests that polar activators (e.g., methanol, ethanol, propylene carbonate) be used at levels of 33 to 50% based on the weight of the organoclay. However, there may be overriding factors that may necessitate significantly different levels of usage. For example, miscibility of the activator with the solvent can be an important factor in determining optimum activator levels. This point is illustrated

in the use of ethanol to activate the dispersion of dimethylbenzyl tallow ammonium bentonite in methyl styrene. An alcohol/methyl styrene mixture at a weight ratio of 10/90 produces an immiscible solvent mixture at room temperature. Attempted dispersion of the organoclay at a concentration of 3 wt % into this mixture produced a hazy dispersion with significant amounts of light scattering, even at high angles. However, when the activator and solvent are made miscible by increasing the ethanol concentration, the organoclay is readily dispersed, despite the high alcohol concentration relative to the weight of the organoclay. This time, a miscible ratio of 18/82 produced a transparent, highly-viscous organoclay dispersion that showed no visible low-angle scattering of light, which are all indications of an exfoliated state.

While solvent miscibility is one factor guiding the choice of an activator, further guidance is available. For example, the electrostatic factor (EF) [14], defined as the product of the dipole moment and the relative permittivity, appears to predict the effectiveness of an activator to promote organoclay swelling. In Fig. 1, the gel volume for an octadecyl ammonium bentonite is plotted as a function of the activator's EF value. The gel volume data are from Jordan [2] and pertain to organoclay swelling in alcohol/toluene mixtures having a 10/90 volume ratio. Jordan's data show that as the chain length of the alcohol is increased, the gel volume asymptotically decreases, approaching that of the organoclay in pure toluene (note: toluene has an EF value of 3.1 [14]). The fact that the gel volume extrapolates to zero with solutes having an EF value of zero suggests that certain types of molecules may actually inhibit organoclay exfoliation. Likewise, choosing a solvent with an EF value of zero (e.g., *p*-xylene) would be expected to have the same deleterious effect on clay dispersion.

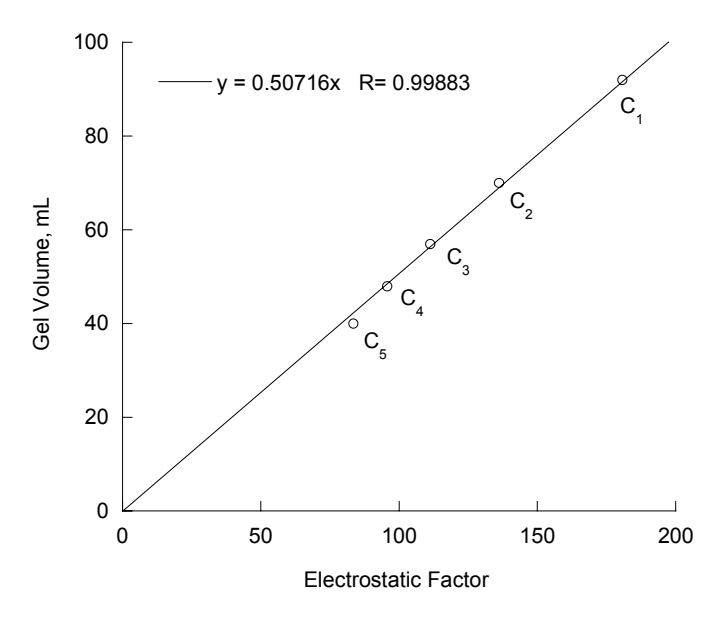


Fig. 1. A plot of gel volume for octadecyl ammonium bentonite in binary mixtures of alcohol-10/toluene-90 as a function of electrostatic factor of the primary alcohol. The gel volume data are taken from the curve fit to the data in Fig. 5 of Jordan [6] and the EF values are from Barton [14].

In the present study, this hypothesis was tested with the use of a cetyltrimethyl ammonium bentonite containing 110 milli-equivalents of quaternary amine per 100 g of clay. Dispersing 0.25 g of cetyltrimethyl ammonium bentonite in 5 mL of toluene produced a translucent dispersion (i.e., tactoid formation), but solvent mixtures of ethanol/toluene (10/90 volume ratio) produced a transparent, stiff gel. However, organoclay dispersions in heptane/toluene mixtures were runny and the clay was clearly flocculated. In this case, the addition of heptane, with an EF value of zero [14], inhibited the exfoliation of the organoclay.

Unfortunately, the most effective activators identified by Jordan (e.g., methanol, ethanol, ethyl acetate) would not be suitable for preparing polyolefin nanocomposites by melt compounding because of their low boiling points and immiscibility with these hydrophobic polymers. Effective activators for polyolefin systems would be compatible with both the organoclay and the polymer. Using high-boiling alcohols like erythritol would not promote exfoliation because of the immiscibility of the highly polar alcohol with polyolefin homopolymers.

A more fruitful method of activation, attempted by others [9-12] would seem to be the use of oligomers and co-polymers. Not only is the higher molecular weight more compatible with the melt processing temperatures of polyolefins, but the higher molecular weight offers the opportunity for enhanced wetting of the organoclay, both in the melt and solid states. However, the use of oligomers as activators does not necessarily guarantee the exfoliation of an organoclay in polymer systems. This point is examined in detail in the next section.

Surface wetting

The importance of this effect can be better understood by examining the contact angles generated between a polyolefin melt and an organoclay surface. With data on the surface tension of the polymer, the contact angle can be estimated from [15]:

$$\cos \theta = 1 - \beta (\gamma_L - \gamma_c) \tag{1}$$

Where θ is the contact angle, β is a constant that ranges between 0.3 and 0.4, γ_L is the surface tension of the polymer melt, and γ_c is the critical surface tension of the organoclay's basal plane. Equation 1 suggests that liquids (e.g., polymer melts) having surface tensions less than γ_c will spontaneously wet the organoclay surface. However, this should not be construed to mean that the wetting liquid will spontaneously wet intra-gallery surfaces. Polymer melts will undoubtedly suffer significant entropy losses when confined within the organoclay gallery. As a first approximation, the critical surface tension of the organoclay can be taken to be 22 mJ·m⁻², which is the value given by Zisman [16] for a –CH₃ crystal surface. The surface tension of the polyethylene melt is reported to be 22.7 mJ·m⁻² at 180°C [17]. The surface energies are probably too close to warrant any significant conclusions from the contact angle calculation. However, as the temperature of the polymer melt is reduced, the surface tension of the polymer

quickly rises and a non-wetting state can be anticipated. For example, at 140° C the interfacial tension of the polymer melt increases to $24.5-26.5 \text{ mJ} \cdot \text{m}^{-2}$ [17]. This rise in surface tension will produce contact angles at the basal plane that are as high as 110 degrees, which are sufficient to cause the organoclay to flocculate and phase separate from the polymer melt.

In the case of polypropylene, which has a surface tension of 21 mJ·m⁻² at 180°C [17], the polymer would spontaneously wet the organoclay surface. However, at room temperature, the surface tension of polypropylene increases to values ranging from 30 to 33 mJ·m⁻². Under these conditions, the amorphous polymer phase would no longer wet the organoclay surface, and we should not expect any improvement in mechanical or gas barrier properties.

One way to avoid the dewetting condition would be to increase the critical surface tension of the basal plane at room temperature. This can be done by sufficiently increasing the chain length of the quaternary amine or the surface modifier, so that the external basal plane is comprised predominately of –CH₂–groups. At room temperature, the critical surface tension of the exposed basal plane would increase to approximately 33·mJ·m⁻² [16], and thereby maintain wetting of the organoclay by the polyolefin.

Thus, the use of oligomeric modifiers would seem to be a rational approach to enhancing the dispersion of organoclays into polyolefins. However, this is dependent upon the oligomer being adsorbed in such a way that the critical surface tension is characteristic of $-CH_2$ — type surfaces; if the oligomer resides deep in the palisade region of the basal surface, the surface will remain in a low energy state at room temperature and phase separation from the polyolefin can be expected.

Unfortunately, olefinic modifiers have thus far produced less than ideal results, as they rarely lead to a significant increase in the basal spacing of the organoclay. For example, Dontula et al. [12] report basal spacings for Cloisite 25A/polyethylene-block-poly(ethylene glycol) intercalates that increased from 2.1 nm to only 2.94 nm. The clay/oligomer ratio was 2:1, and the intercalate was prepared by melt mixing. While the fraction of the oligomer incorporated as an intercalated phase was not reported, it is fair to conclude that the 0.8 nm increase in basal spacing suggests that, at best, only a bilayer was actually adsorbed onto the clay. The polar poly(ethylene glycol) group is likely associated with the quaternary ammonium ion, while the polyethylene group is probably associated with naturally hydrophobic siloxane sites. The question of whether further clay swelling was limited by either thermodynamic or kinetic factors (or both) warrants further investigation.

Organoclay intercalation

In the present study, a different approach to intercalation by polyethylene-*block*-poly(ethylene glycol) was attempted to promote surface activation of the organo-clay (note: intercalation and activation can be considered synonymous only when the intercalate is capable of exfoliation). To eliminate kinetic and thermodynamic

factors that might retard or prevent oligomer intercalation, the organoclay was first dispersed in toluene and exfoliated by organoclay activation with ethanol. This ensures that the oligomer will have direct access to the largest possible number of exposed basal surfaces. Also of importance is the fact that toluene can solvate both the ditallow chains and the oligomer. No doubt, relying on the oligomer to wet and solvate the external –CH₃ surface of the organoclay will be as difficult to achieve as direct wetting by a polyolefin.

The toluene/ethanol/water and toluene/water azeotropes were sequentially distilled off before the oligomer was added to the clay dispersion. Removing as much water as possible from the organoclay surface was deemed necessary to promote solvation of the organoclay surface by the oligomer.

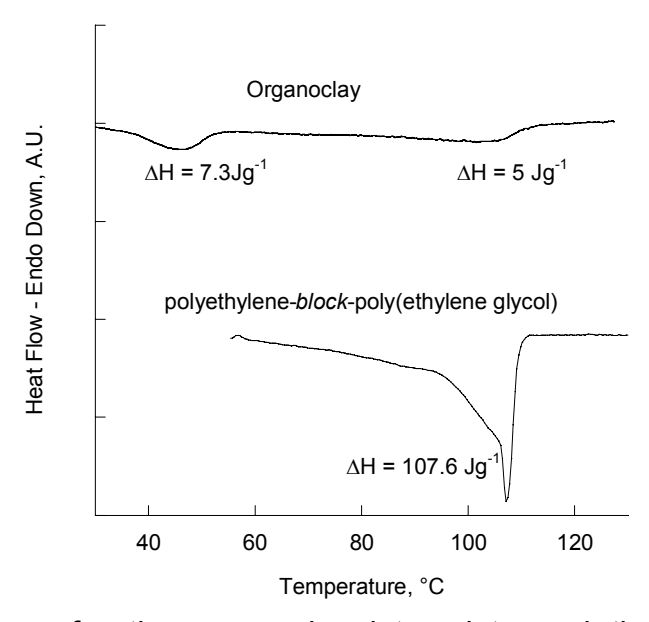


Fig. 2. Melt curves for the organoclay intercalate and the neat oligomeric activator.

By separately measuring the crystallinity of the oligomer, it was possible to estimate the amount of oligomer remaining intercalated within the organoclay galleries after solvent removal. The heat of melting (ΔH_m) for the polyethylene-block-poly(ethylene glycol) crystal phase was measured by DSC, and its value was compared with the corresponding ΔH_m value of the organoclay intercalate. In Fig. 2, the heating curves for the pure oligomer and the intercalate are compared. While the ΔH_m value for the pure oligomer is 107.6 J·g⁻¹, its corresponding value, when associated with the organoclay, is only 23.8 J·g⁻¹ (note: this value was normalized for the weight fraction of the oligomer in the organoclay/oligomer mixture). Thus, the fraction of oligomeric activator actually associated with an organoclay surface was estimated to be 0.78 (e.g., 1–23.8/107.6). The remainder of the oligomeric activator is evidently present as a discrete, crystal phase.

Two additional intercalation methods were attempted—a second solvent approach and a direct melt-mixing process. In the solvent-mediated approach,

the organoclay was dispersed in *o*-xylene and the oligomer was added at a weight ratio of 1:1 together with tetramethoxysilane (TMOS), a high-boiling activator identified by Jordan [6]. The dispersion was heated to 140°C for 30 min, and a small amount of mineral oil was added before removing the solvent. Mineral oil has a low surface tension at all processing temperatures, and was added to maintain a state of solvation for the –CH₃ surface after solvent removal. This approach produced a colorless, transparent intercalate that liquefied at temperatures above 100 °C.

In the melt-mixed process, the organoclay was combined with an equal weight of the oligomer and mixed for 5 min by hand on a hot plate at 140°C. The XRD patterns for the two intercalated samples are compared in Fig. 3, and confirm that direct-melt compounding produces only a minor degree of intercalation, while the solvent approach yields a nanocomposite with no detectable basal spacing. In the absence of TMOS, addition of the oligomer to the clay/xylene dispersion failed to produce an exfoliated product, confirming that a low-molecular-weight polar activator is crucial to reaching an exfoliated condition. In other words, solvent mixtures (e.g., o-xylene/TMOS) appear to provide sufficient reduction in the interfacial tension between the organoclay and the oligomer, both at the mineral plane and the external –CH₃ plane, to promote exfoliation.

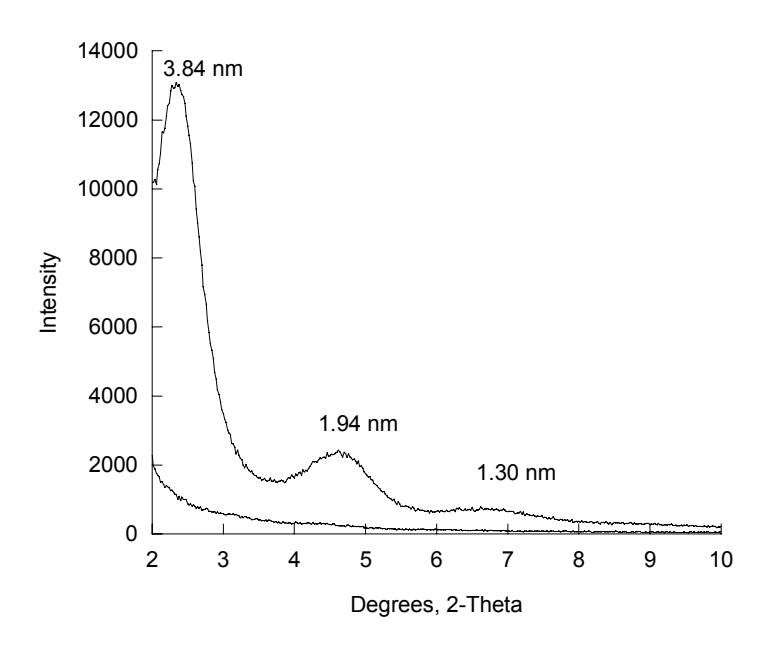


Fig. 3. XRD profiles for the melt-intercalated organoclay (top curve) and the solvent-mediated intercalate (bottom curve). Both organoclays were prepared with polyethylene-*block*-poly(ethylene glycol) at a clay/oligomer ratio of 1.

Intercalate dispersion in HDPE

The organoclay produced from the toluene/ethanol-mediated intercalation was compounded into HDPE to ascertain its ability to affect gas barrier properties,

particularly for water vapor. Because the organoclay intercalate has a much higher viscosity than the polymer melt, it was felt that the melt mixing would progress most efficiently by incrementally adding the polymer melt to the activated organoclay, thereby gradually reducing the viscosity of the system. The initial polymer addition was made while maintaining the organoclay as the continuous phase. The gradual clay dilution was continued until a final concentration of approximately 0.3 wt% (i.e., ash content) was attained. While typical organoclay concentrations of 5 to 10 wt% have been used in numerous nanocomposite studies [18], the clay concentration used in the present study is more in line with that of other polymer additives, such as colorants, clarifiers, and stabilizers, rather than conventional fillers like talc and kaolin.

Compression-molded films of the nanocomposite and the pure polymer were prepared under identical melt/cool conditions. The most obvious difference between the nanocomposite and the HDPE reference was the extraordinary transparency of the nanocomposite films. The normal spherulitic structures of HDPE, which are clearly visible under polarized-light microscopy, were completely absent in the nanocomposite. For example, scanning electron microscopy images of the films are shown in Fig. 4, and except for some surface debris, the nanocomposite surface is featureless. The absence of visible spherulites in the nanocomposite suggests that extensive nucleation, promoted by the organoclay, has taken place. In other words, the nucleation density became so large that spherulite growth was arrested by impingement on neighboring spherulites before reaching a size large enough to either scatter visible light or become visible by scanning electron microscopy. While nucleation behavior has been reported in previous HDPE nanocomposite studies [10, 12], this is the first reported instance of an organoclay being capable of clarifying HDPE.

Differential scanning calorimetry measurements were performed to estimate the extent of polymer crystallization in the nanocomposite. While it is known that high clay concentrations can actually inhibit HDPE crystallization [12], this was not expected to be the cause of the increased film clarity because of the low clay concentration used in the present study. The results from the DSC measurements are shown in Fig. 5, where the heating curve for the nanocomposite is compared with that of the reference polymer. The ΔH_{m} values for the melt transitions of the two polymer samples are virtually identical, confirming that the clarity of the nanocomposite is due to a significant increase in heterogeneous nucleation, rather than a loss in crystallinity. By comparing the ΔH_{m} values from the DSC data in Fig. 5 with the literature [19] value for the polyethylene crystal phase (i.e., ΔH_{m} = 293 J·g $^{-1}$), it was possible to estimate the degree of crystallinity in the nanocomposite. This calculation yields a value of 63% crystallinity for the HDPE reference film and 61% for the nanocomposite film.

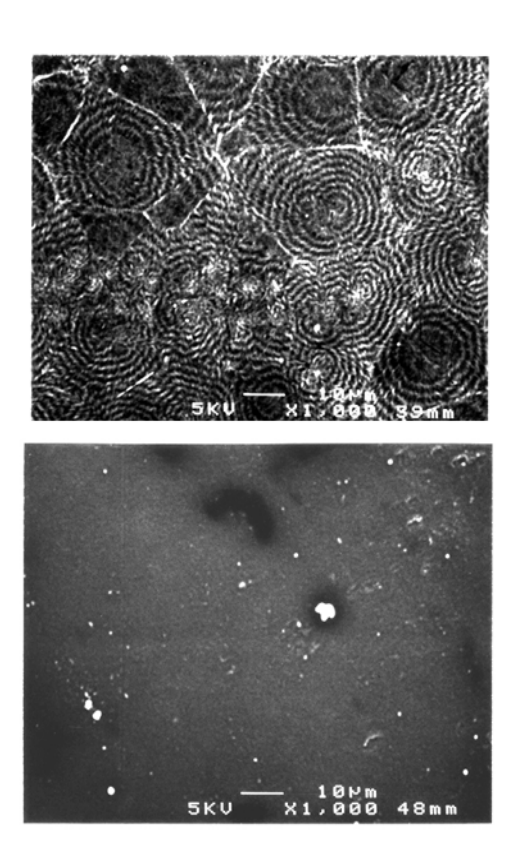


Fig. 4. SEM images of the HDPE reference (top) and the nanocomposite (bottom). Except for some surface debris, the nanocomposite surface is completely void of any surface structures, including spherulites.

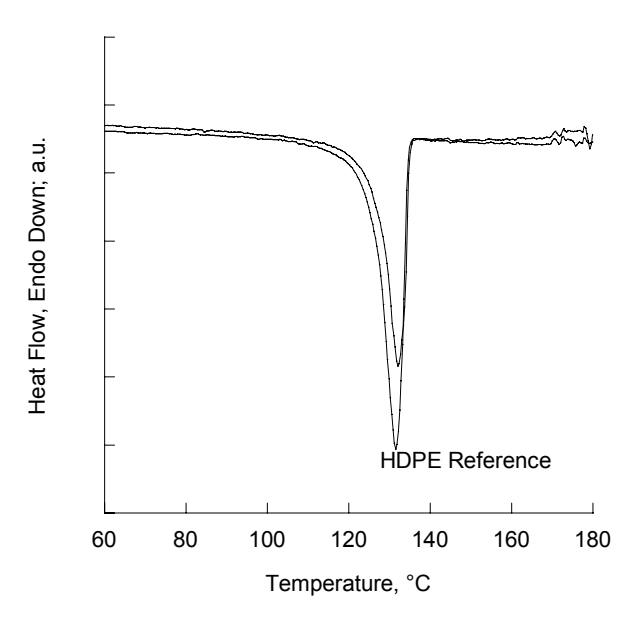


Fig. 5. Heat curves for the neat polymer (bottom curve) and the nanocomposite; the heats of melting were 184.8 and 179.5 $J \cdot g^{-1}$, respectively. The melt transition peak occurred at 132°C.

Gas transmission measurements

While an organoclay may reduce gas transmission through a tortuous path mechanism, it should also be possible to increase the gas barrier by sufficiently reducing spherulite size, thereby inducing a tortuous path around the nanoscale spherulites. This effect would be most pronounced for semicrystalline polymers like HDPE and polypropylene, which have a relatively high degree of crystallinity. Additionally, since the crystallinity and hence the volume fraction of the amorphous polymer phase are essentially unchanged in the HDPE nanocomposite, the higher specific surface area associated with the polymer crystal phase would reduce the thickness of the amorphous interphase surrounding the smaller spherulites. As the amorphous region becomes narrower, chain mobility is reduced. In the extreme, the passages can become so thin that gas transmission becomes hindered [20].

To determine if a hindered diffusion state was produced, both oxygentransmission-rate (OTR) and water-vapor-transmission-rate (WVTR) measurements were performed on the nanocomposite film and compared with measured values for the reference polymer (note: in the absence of hindered diffusion, the reduction in transmission should be the same for all gases). The oxygen transmission curves for the nanocomposite and reference HDPE films are shown in Fig. 6. Oxygen transmission rates were calculated from the steady-state portions of the transmission curves and then normalized for film thickness. The resulting permeabilities for the neat polymer and the nanocomposite were 98.3 and 42.9 cc·mil/100 in²·d·atm, respectively. Thus, the oxygen permeability was reduced by approximately 55% with the addition of less than 0.5 wt% organoclay. This can be compared with published data from the Nanocor website [21], which reports a 21% reduction in oxygen permeability for HDPE nanocomposites containing 6 wt% organoclay, a concentration reported by Nanocor to be an optimum loading. Water vapor transmission data are not reported on the Nanocor website for polyolefin homopolymers. In fact, a search of the literature failed to find any report of an increased water vapor barrier in nanoclay/HDPE systems.

Results for WVTR measurements are shown in Fig. 7. The reduction in WVTR was slightly greater than that for oxygen, suggesting that something other than a simple tortuous path mechanism is at work. The water vapor permeabilities for the neat polymer and the nanocomposite were 0.065 and 0.02 g·mil/100 in²·d·atm, respectively, which represents a 70% reduction. As in the OTR data, an increase in the lag time (i.e., the *x*-axis intercept from the steady-state portion of the pressure vs. time curve) was observed. Attributing the barrier improvement to an increased tortuous diffusion path around the organoclay platelets and some degree of hindered diffusion would seem to be reasonable.

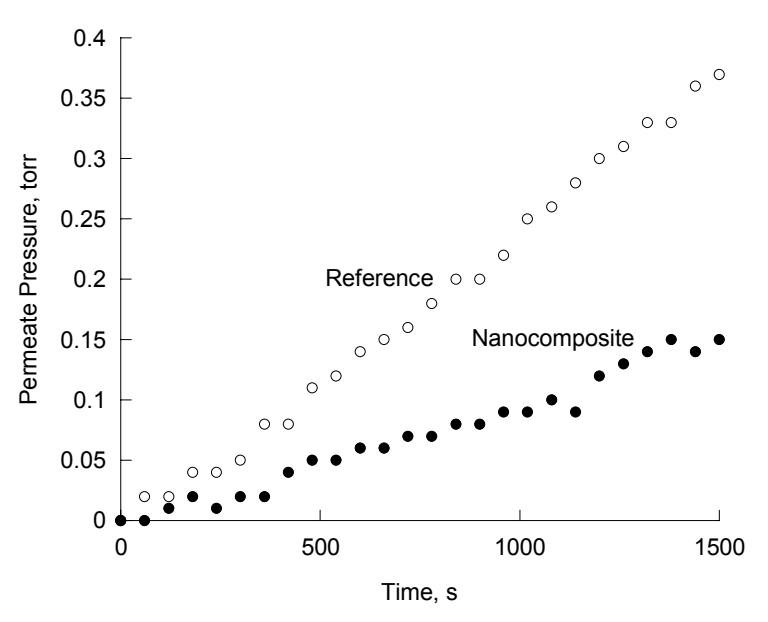


Fig. 6. Oxygen transmission across HDPE films at 30°C, 0 % humidity. Steady-state permeabilities for the nanocomposite and the reference films are 42.9 and 98.3 cc·mil/100 in²·d·atm, respectively.

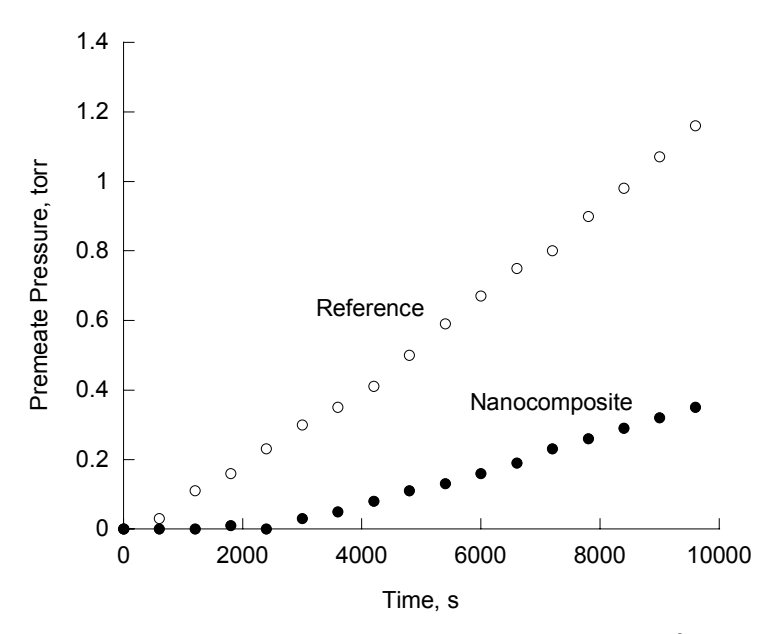


Fig. 7. Water vapor transmission across HDPE films at 30°C, 100 % humidity. Steady-state permeabilities for the nanocomposite and the reference films are 0.02 and 0.065 g·mil/100 in²·d·atm, respectively.

This view is further supported by closer examination of the lag time (θ), which provides an estimate for the diffusion coefficient (D) (i.e., θ = I 2 /6·D; where I is the film thickness). Using the water vapor transmission data, the calculated values for the reference polymer (D_o) and the nanocomposite (D) are 1.9×10^{-8} and 0.65×10^{-8} cm²·s⁻¹, respectively. If the change in diffusivity were due solely

to tortuousity around the clay platelets, the ratio in diffusivities would be expected to be described by the following relationship [22]:

$$\frac{D}{D_a} = \frac{1}{1 + \alpha^2 \phi^2} \tag{2}$$

where α is the aspect ratio of the clay platelets and Φ is the volume fraction of the clay in the nanocomposite.

Thus, the diffusion coefficients obtained from the lag time can be used to estimate α . From the OTR and WVTR data, α was estimated to be just over 1000, a value that is considerably larger than the commonly accepted range for exfoliated montmorillonites (i.e., 100–500). Even when excluding the volume fraction of the polymer crystal phase in the calculation of Φ , the aspect ratio is still quite large at 550. A number of this magnitude would require complete exfoliation and perfect platelet alignment within the nanocomposite film, which is an extremely optimistic situation and probably not realistic.

Some type of specific interaction of the gas, especially for water vapor, with the clay surface is another possible explanation for the large barrier improvement. A reversible reaction, having an equilibrium constant of K, with an immobile phase such as the clay platelets, would indeed lead to an increase in the time lag by a factor of (1 + K) [22]. However, the steady-state flux would not be affected and must remain identical to that of the pure polymer. This is also true when the reaction is irreversible. Since the steady-state flux for both water vapor and oxygen were reduced relative to the pure polymer, the increase in the breakthrough time cannot be attributed to either adsorption or reaction at the clay surface.

It is likely that the gas barrier improvement is due to a combination of factors, including the tortuous diffusion path around the clay platelets and the polymer crystal phase, together with some hindered diffusion through the amorphous interphase between the polymer spherulites. This explanation is consistent with differing degrees of barrier improvement between oxygen and water vapor.

Conclusions

Significant improvements in the oxygen and water vapor barrier were observed for HDPE nanocomposites at a clay (ash) loading of only 0.3 wt%. This organoclay concentration is consistent with that of other polymer additives, such as clarifiers, stabilizers, and dyes. A significant improvement in polymer clarity was observed without a significant loss in polymer crystallinity. The improved gas barrier of the nanocomposite can be attributed to an increased tortuous diffusion path around the clay platelets and the reduced polymer spherulites, together with hindered diffusion through the amorphous interphase surrounding the polymer spherulites. Furthermore, spherulite size was reduced sufficiently to eliminate scattering of visible light from the nanocomposite.

Organoclay dispersion into the polymer was aided by the use of an oligomeric activator, which was adsorbed onto the organoclay via a solvent technique. To promote adsorption of the oligomer onto the organoclay, it was necessary to include a polar activator such as ethanol or TMOS. From an examination of literature data, the efficiency of the polar activator was shown to be a linear function of the molecule's electrostatic factor.

An analysis of published surface tension data indicates that polyolefin melts, especially polypropylene, can wet the external organoclay surface, but a state of non-wetting quickly arises as the polymer melt cools. Even minor cooling (e.g., 140°C) is sufficient to produce a large contact angle between the polyethylene melt and the organoclay surface. An oligomeric activator was used to modify the organoclay surface and increase its surface tension, thereby maintaining a dispersed state within the polymer melt as it cooled.

Experimental part

Materials and methods

The organoclay was prepared from a Na⁺ montmorillonite (Cloisite Na, Southern Clay Products). The clay was dispersed in deionized water at a solids concentration of 2.5 wt%. The edge of the clay was treated with the ammonium salt of 1hydroxy-dodecane-1,1-diphosphonate (Solutia) at a concentration of 0.6 wt % relative to the weight of the dry clay. This preparation detail differs from previously described preparations [13], in that the alkyl diphosphonate concentration was reduced from 3 wt% to 0.6 wt%. This change was initiated to plant hydrocarbon chains on the edge of the clay platelets while at the same time minimizing the possibility of charge reversal. The temperature of the clay dispersion was raised from room temperature to 70°C, after which the basal surfaces of the clay platelets were treated by ion exchange with 110 milli-equivalents of dimethyl dihydrogenated tallow ammonium chloride (Arquad 2HT-75, Akzo Nobel) per 100 g clay. Combined with the quaternary amine were (a) poly(propylene glycol) with a molecular weight of 1000 at a concentration of 4 g per 100 g of clay, and (b) 2000 ppm Irganox B225 (Ciba Specialty Chemicals Co.) (contains 50% tris(2,4di-(tert)-butylphenyl) phosphate and 50% tetrakis[methylene(3,5-di-(tert)-butyl-4hydroxyhydrocinnamate) methane] relative to the weight of the clay. After completion of the ion exchange reaction, the organoclay was filtered and then washed with deionized water. The organoclay was recovered as a pressed filter cake containing approximately 65 wt % water. The preparation of the organoclay intercalate involved drying the wet filter cake overnight at 40°C and dispersing the dried clay in 1 L of toluene at a solids concentration of approximately 6 wt%. Ethanol, in an amount equal in weight to the organoclay, was used as a polar activator to aid clay dispersion and promote exfoliation. The solvent dispersion was heated in a round-bottom flask, under nitrogen, until the last of the toluene/ethanol/water and then the toluene/water azeotropes were removed and the expected boiling point (i.e., 110°C) of toluene was reached. The organoclay surface was then modified by the addition of the oligomeric surfactant polyethylene-block-poly(ethylene glycol) (M_n 1400; HLB 10.0, Sigma-Aldrich) to the hot organoclay dispersion. The oligomer was added at a ratio of 20 wt% relative to the weight of the organoclay. An antioxidant (0.3 wt% 2,5,7,8-tetramethyl-2-(4',8',12'-trimethyltridecyl)-6-chromanol, Aldrich) was added to the toluene dispersion to later protect the poly(ethylene glycol) moiety during the clay/polymer processing steps. Mixing was continued for 30 min under reflux, and then the toluene was removed by distillation under a nitrogen flow. It should be noted that the dried material was black.

The modified organoclay was diluted with HDPE (Equistar) by slowly adding the polymer, one pellet at a time, and melt mixed to a final clay (ash content) loading of 0.3 wt%. Overall, approximately 25 mg of activated organoclay were diluted with approximately 5 g of polymer. The mixing was done by hand, using a spatula and heating the material on a hotplate to approximately 170°C. The organoclay intercalate dispersed rapidly when mixed in this manner, almost instantly becoming colorless and transparent with the initial addition of polymer.

Compression-molded films were produced at a melt temperature of 160° C. A reference set of HDPE films were prepared in an identical manner to ensure that the nanocomposite and the reference were exposed to the same melt/freeze history. Scanning electron microscopy (SEM) images were obtained using a JEOL microscope with polymer samples that were carbon coated using a variety of treatment times (10 s to 3 min) to ensure that surface details were not masked by the carbon layer. Differential scanning calorimetry (DSC) measurements were performed with a Perkin-Elmer Pyris 1 calorimeter under an argon atmosphere and a scan rate of 10° C min⁻¹. Basal spacings were measured by X-ray diffraction (XRD) with a Rigaku diffractometer with Cu K α radiation, λ = 1.541 Å. Gas transmission rates were measured using a diffusion cell technique, following ASTM D 3985-9 on compression molded polymer films. The measurements were carried out at 30°C on films that had been aged at least one month before the measurements. The gas transmission measurements included oxygen and water vapor.

Acknowledgements

This work was supported by the DOE's FreedomCAR & Vehicle Technologies Office under contract No. W-31-109-ENG-38 and by the Chemical Engineering Division, Argonne National Laboratory. The alkyl diphosphonate was provided by Dr. Tim Hirzel, at Solutia.

References

- [1] Hauser, E. A. *Silicic Science*; D. Van Nostrand Company: New York, p.176, **1955**.
- [2] Jordan, J. W. J. Phys. Colloid Chem. 1949, 53, 294.
- [3] Jordan, J. W.; Hook, B. J.; Finlayson, C. M. *J. Phys. Colloid Chem.* **1950**, *54*, 1196.
- [4] Jordan, J. W.; Williams, F. J. Kolloid Zeitschrift 1954, 137, 40.

- [5] Theng, B. K. G. Formation and Properties of Clay-Polymer Complexes; Elsevier: New York, **1979**.
- [6] Iannicelli, J. Minerals & Metallurgical Processing 1991, 8, 135.
- [7] Usuki, A.; Kato, M.; Okada, A.; Kurauchi, T. *J. Applied Polym. Sci.* **1997**, *68*, 137.
- [8] Usuki, A.; Mizutani, T.; Fukushima, Y.; Fujimoto, M.; Fukumori, K.; Kojima, Y.; Sato, N.; Kurauchi, T.; Kamigaito, O. U.S. Patent 4,889,885, Dec. 26, **1989**.
- [9] Kawasumi, M.; Hasegawa, N.; Kato, M.; Usuki, A.; Okada, A. *Macromolecules* **1997**, *30*, 6333.
- [10] Ishida, H.; Campbell, S.; Blackwell, T. Chem. Mater. 2000, 12, 1260.
- [11] Dontula, N.; Blanton, T. N.; Majumdar, D. U.S. Patent 6,841,226, Jan. 11, **2005**.
- [12] Gopakumar, T. G.; Lee, J. A.; Kontopoulou, M.; Parent, J.S. *Polymer* **2002**, *43*, 5483.
- [13] Chaiko, D. J.; Leyva, A. A. Chem. Mater. 2005, 17, 13.
- [14] Barton, A. F. M. *CRC Handbook of Solubility Parameters and Other Cohesion Parameters*; CRC Press: Boca Raton, FL, pp. 171–173, **1985**.
- [15] Adamson, A. W. *Physical Chemistry of Surfaces*; John Wiley & Sons: New York, **1976**.
- [16] Zisman, W. A. ACS Adv. Chem. Ser. 1964, 43, 1.
- [17] Kwok, D. Y.; Cheung, L. K.; Park, C. B.; Neumann, A. W. *Polymer Eng. Sci.* **1998**, *38*, 757.
- [18] Pinnavaia, T. J.; Beall, G. W., Eds. *Polymer-Clay Nanocomposites*; John Wiley & Sons: New York, **2000**.
- [19] Runt, J. P. *Encyclopedia of Polymer Science and Engineering*; John Wiley & Sons: New York, vol. 4, p. 487, **1985**.
- [20] Klopffer, M. H.; Flaconnèche, B. Oil & Gas Science and Technology 2001, 56, 223.
- [21] Nanocor. *Polyolefin Nanocomposites*, Technical Data Sheet, P-807; Arlington Heights, IL, **2002**.
- [22] Yang, C.; Nuxoll, E. E.; Cussler, E.I. AIChE Journal 2001, 47, 295.